Article:
Wahle, M orcid.org/0000-0002-2241-9975, Snow, B, Sargent, J et al. (1 more author) (2019) Embossing Reactive Mesogens: A Facile Approach to Polarisation-Independent Liquid Crystal Devices. Advanced Optical Materials, 7 (2). ARTN 1801261. ISSN 2195-1071

https://doi.org/10.1002/adom.201801261

Embossing Reactive Mesogens: A Facile Approach to Polarisation-Independent Liquid Crystal Devices

*Markus Wahle, Benjamin Snow, Joe Sargent and J. Cliff Jones**

Reactive mesogens (RMs) have been used in a wide variety of applications, from retardation plates for OLED screens, liquid crystal phase stabilisation, optical or electrically active elastomers to novel optic components. They can be processed as standard liquid crystals and subsequently polymerised to stabilise both shape and anisotropic properties. However, creating complex shapes while maintaining good alignment of the RM optical axis can be a challenge. In the present work, embossing is used to replicate a wide variety of RM structures in several electro-optic devices. A novel device geometry is proposed where a polarisation-independent lens is formed by opposing birefringent Fresnel zone plates embossed in aligned RM. The RM forms the optical elements and alignment layers for an index-matched liquid crystal, arranged to form the twisted nematic configuration. Low voltages switch the device between non-focusing and focusing states. After characterising lens efficiency and beam properties, the method is used to fabricate a switchable multi-level Fresnel zone plate with optical efficiencies beyond 50 %, and theoretically able to produce polarisation independent lenses with efficiencies approaching 100% from a single structure. Finally, manufactured polarisation-independent gratings and microlens arrays are presented using the method to illustrate the wide range of applicability.

Dr. M. Wahle, Prof. J. C. Jones
Soft Matter Physics, School of Physics and Astronomy, University of Leeds, Leeds, LS2 9JT, UK
J.C.Jones@leeds.ac.uk
Dr. B. Snow, J. Sargent
Merck Chemicals Ltd, University Parkway, Chilworth, Southampton, SO16 7QD, UK

Keywords: polarisation-independent devices, liquid crystals, reactive mesogens, embossing

1 Introduction

Polymerisable liquid crystals, known as reactive mesogens (RMs), have proven to be versatile materials with applications as high retardation optical films for use in liquid crystal displays (LCD) and organic light emitting displays (OLED), as stabiliser for complex liquid crystalline phases such as blue phases [1, 2] and, more recently, as actuating liquid crystal elastomers [3-7] and for an ever increasing list of diverse applications [8]. As for standard nematic liquid crystals (LCs), RMs are anisotropic and the director field can be controlled by geometry and surface treatment. However, RMs can be polymerised to retain their shape and anisotropic properties. Typically, the molecular design of RMs is based on nematic LCs, but with acrylate groups included in the end-chain design, to enable polymerisation of the material. This can be utilized for tailored actuators or specific anisotropic optical components. However, this requires precise spatial structuring of RMs while maintaining good alignment; this remains a challenge in processing.

The simplest device fabrication method is to polymerise RMs in a cell and remove the resultant polymer film after polymerisation [9]. This of course is limited to the creation of planar films. Analogue to isotropic resins, direct writing processes [10, 11] can be used to produce structured films but these techniques are in general slow and therefore not suitable for high volume production. Further, as the polymerisation of RMs relies on acrylate groups, the processing has to be performed in an oxygen-free atmosphere to avoid inhibition of the cure. These issues can be circumvented by employing imprinting techniques, such as nano-indentation lithography (NIL) [12]. Although such methods can reproduce sub-micron features with fidelity, they have the drawback of creating unwanted additional

layers beneath the copied structure, called offset. Offset is a serious problem in electrooptic devices as it causes unnecessary voltage drop that can be significant, given the large difference in permittivity between the polymer layer and contacting liquid crystal. Also, the offset is rarely uniform, and causes large switching variations over the device. Thus, optical elements formed using standard NIL previously are often used beneath the electrode layer or even externally to the liquid crystal cell, thereby leading to more complex designs and additional losses and inefficiencies.

In this work, an embossing technique is developed to structure and align reactive mesogens to form anisotropic components with varying shapes. Embossing enables large scale reproduction of components with high accuracy and without offset, thereby allowing more complex, novel switchable optical elements to be formed. Due to the high fidelity, this technique is used for the nanometre precise reproductions of isotropic optical components such as sub-micrometre gratings [13, 14]. We show that the technique can be adapted to create arbitrary structured anisotropic components using reactive mesogens. As an application, we employ embossed birefringent optical elements to build novel polarisation-independent switchable optical devices [15], also being reported for the first time.

Achieving polarisation-independence in liquid crystal-based devices is a general challenge that applies to many different optical elements like beam steerers, optical gratings and lenses. The latter has attracted much attention recently for applications ranging from contact lenses [16, 17] over cameras [18] to augmented or mixed reality [19]. However, most of the realisations of LC lenses are dependent on the polarisation of light [20-22], which limits their efficiency significantly for many use cases. There exist a few approaches to solve this issue, but those solutions lead to bulky devices [23, 24], need high driving voltages [25 - 28], or they are inherently limited in efficiency [23, 29 - 31].

As a first example for polarisation-independent lenses, we employ two embossed birefringent Fresnel zone plates (FZPs), which are assembled to form a liquid crystal cell. The optical axes of the two FZPs are orthogonal, which leads to a twisted nematic configuration when filled with a nematic liquid crystal.

The ordinary and extraordinary refractive indices of the LC are index matched to the RM, which enables switching from a non-focusing to a focusing state. We extend this approach to multi-level Fresnel lenses to overcome the efficiency limits of the binary structure. To prove the wide applicability in the field of optics, we further show examples for polarisation-independent optical gratings and microlens arrays.

2 Embossing of Reactive Mesogens

A Fresnel zone plate relies on diffraction effects to focus light at a focal point. Light transmitted from a collimated source and through the FZP is focused by phase shifting light that would interfere destructively in the focal point by a half wavelength. This leads to the partitioning of the plate into the eponymous zones. From simple geometric arguments and the interference condition, the zone radii r_m are given by:

$$r_m = \left[m\lambda\left(f + \frac{m}{4}\lambda\right)\right]^{1/2}, \qquad (1)$$

where m is the number of the ring, f the nominal focal length and λ the wavelength.

The process of manufacturing the reactive mesogen embossed Fresnel zone plate is shown in **Figure 1**. A master structure was made by direct laser writing into photoresist. The master is coated with a release layer and is moulded using UV-curable photo-polymerisable material. This material is on a flexible PET film, which is a prerequisite for the embossing process. The negative mould is then coated with a polyvinyl alcohol (PVA) alignment layer and rubbed, to impart the optical axis of the final birefringent optical element. Reactive mesogen is deposited onto one side of ITO-covered glass, which has been pre-treated with a rubbed polyimide alignment layer. The rubbed mould is placed on the liquid RM and embossed using a rubber roller. In all of the instances used in the current work, the rubbing direction of both the glass slide and the mould were parallel. After UV-curing the RM, the mould is removed and a copy of the master in aligned RM is obtained. More details on the processing are given in the experimental part.

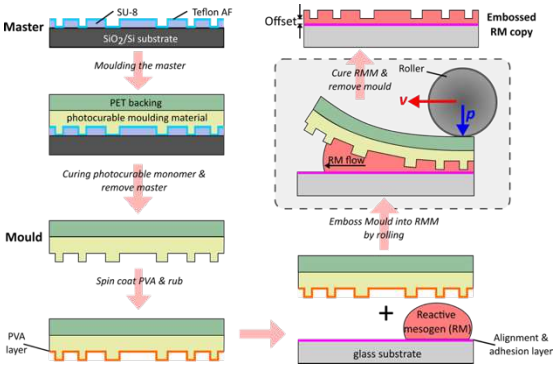

Figure 1*. Flow diagram of the manufacturing process. A detailed description can be found in the text below. Highlighted part shows the embossing steps performed with roller velocity v and under pressure p.*

If the embossing process shown in Figure 1 is optimized, the sample is free from offset. This is facilitated by direct contact of the mould with the substrate, which can be obtained by adjustment of roller speed and pressure between the roller and the sample, the viscosity of the photopolymer, and the radius and shore hardness of the embossing roller [12]. The zero-offset-condition is crucial in electrooptical devices to avoid unnecessary voltage drops and large electrical variations over a device. Other imprint technologies always lead to some offset regardless of how high the pressure is, because the liquid photopolymer is prevented from flowing around a rigid structured element. With embossing, the structured element is on a flexible film, allowing the liquid resin to be pushed from one side of the substrate to the other, filling in the gaps formed between the substrate and the film.

3. Novel Polarisation Independent Liquid Crystal Lens

The ability to provide a simple structured birefringent element on the internal surface of an electro-optic device offers the potential for many novel uses. Examples used here include the polarisation-independent Fresnel lens shown in Fig 2. The device consists of two substrates each with ITO electrodes and a Fresnel zone plate embossed onto it. As stated above, the lensing of the Fresnel zone lens relies on the alternating phase shift of $\pi/2$ thus it does not matter which zones, even or odd, exhibit this phase change. For better device performance, it is advantageous to use complementary structures for the two opposing substrates. For example, this helps ensure that the switching field is uniform across the device with different voltages applied to the electrodes. The reactive mesogen layers are homogeneously aligned and the optical axes of the RM substrates arranged to be perpendicular to each other. On filling, the director of the contacting nematic liquid crystal aligns parallel to the local director of the RM structure. Hence, the director takes up the twisted nematic configuration due to the perpendicular alignment of the two lens substrates. The employed liquid crystal is index matched to the RM, for both the ordinary and extraordinary indices.

The operating principle is summarized in **Figure 2**. In the field-off state, incident collimated light does not experience any distortion of the phase front as the reactive mesogen and the liquid crystal have the same (or very similar) ordinary and extraordinary refractive indices. Hence, incident light will remain collimated without focusing, regardless of the incident polarisation. The only effect is

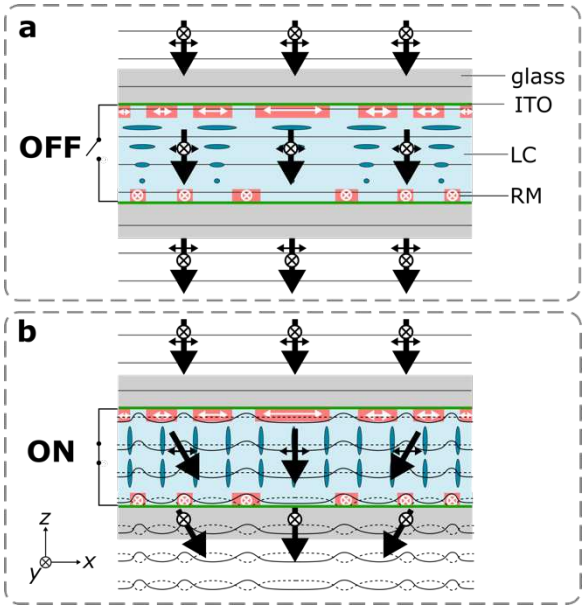

Figure 2. *Principle of operation of the switchable Fresnel lens. (a) OFF-state: Reactive mesogens (RM) and liquid crystal (LC) are index matched, therefore a plane wave passing through the device is not refracted and remains collimated. (b) ON state: Due to reorientation of the liquid crystal an index mismatch is induced between the extraordinary indices of the surface and liquid crystal, causing light to be focused. In-plane polarisation is focused by the top substrate, out-of-plane polarisation at the bottom.*

that due to the twisted nematic geometry, x-polarised light is converted to the y-polarisation and vice versa. The use of the complementary structures on the top and bottom structures is intended to compensate for imperfect index matching. A spatial variation in the optical phase occurring at the top due to index mismatch will be compensated at the complementary places at the bottom.

In the field-on state at sufficient voltages (i.e., higher than the critical, Fréedericksz threshold voltage), the polarisation conversion no longer occurs, and the output polarisation is identical to the input polarisation. The reorientation of the director to a homeotropic state further stops the index matching and lensing at the top and bottom substrates emerges. Specifically, x-polarised light experiences this index mismatch on the top lens while y-polarised light is influenced by the bottom substrate. Hence, lensing for both polarisations is achieved by this Fresnel zones plate cell. Again, the complementary design of the Fresnel zone cell helps in achieving a more homogeneous electric field distribution at constant exposure times. (e-h) Assembled cell with director of both substrates perpendicular to each other. Unfilled cell between crossed polarisers in (e) a 45° angle with respect to polariser, (f) 0° angle. Filled cell (TN like) cell between (g) crossed polarisers and (h) parallel polarisers.

Figure 3 shows polarising optical micrographs of the RM embossed normal (a, b) and complementary (c, d) Fresnel zone plates (FZPs) with 5 mm diameter designed for a focal length of 200 mm at a wavelength of 594 nm. Both structures are accurate reproductions of the master and exhibit very good alignment of the cured RM (for surface profile measurements see **Figure S1** and **Figure S2**, supplementary information). The dark regions

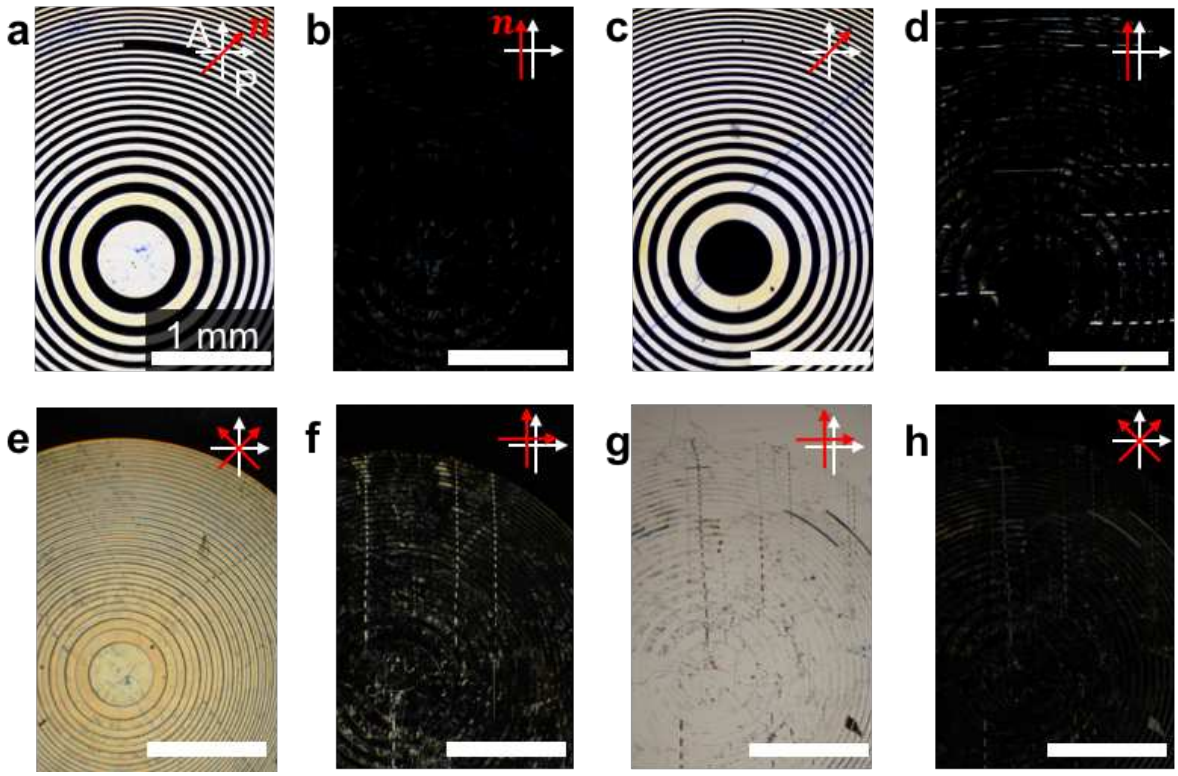

Figure 3. *(a-d) Reactive mesogens embossed substrates. (a, b) Normal structure between crossed polarisers with director in a (a) 45°and (b) 0° angle with respect to polariser. (c, d) Complementary structure. Images are recorded throughout the device, which reduces the operational voltage. The phase shift adopted due to the liquid crystal should therefore be constant throughout the lens so that the transverse phase modulation is solely determined by the reactive mesogen. It should be mentioned that the presented technique of achieving polarisation-independence is not limited to Fresnel zone plates but can be extended to a wide range of optical components, which will be shown later.*

between the RM rings confirm that the embossing process produces structures with zero offset as there is no visible birefringence. The dark state in Figure 3d reveals some minor imperfections that are most likely caused by the rubbing process of the mould and transferred to the RM copy. The normal and complementary FZPs are assembled into a cell with the director of the substrates being perpendicular to each other. The unfilled state of the cell is displayed in Figures 3e and 3f. Due to the complementary design, the cell appears almost homogeneously bright between crossed polarisers if the director assumes a 45° angle to the polariser (Figure 3e). Placed parallel to the polarisers, the sample exhibits a good dark state (Figure 3f). Filling the cell with a liquid crystal leads to a 90° twisted nematic configuration, which appears bright between crossed polarisers (Figure 3g) and dark between parallel polarisers (Figure 3h). This confirms that the alignment of the RM is transferred well to the liquid crystal. A cell gap of 23 µm and a birefringence of the RM and LC of $\Delta n = 0.14$ (589 nm, 25°C) ensures good polarisation conversion, as it is close to the sixth Gooch-Tarry minimum [32].

Figure 4a, b shows a collimated Gaussian beam with diagonal polarisation (with respect to the principle axes of the cell) transmitted through the Fresnel zone plate cell. All experiments are performed with a HeNe laser at 594 nm at room temperature. In the off-state, the beam remains collimated, however, small distortions arise from errors in the filled FZP lens. In the on-state, light is focused to a central spot.

Figure 4(c) shows the efficiency of the device for different input polarisations (for measurement setup see **Figure S3**, supporting information). The efficiency saturates to similar values of approximately 33 % independent of the polarisation. However, while the horizontal polarisation saturates rapidly, the vertical polarisation starts out similar at low voltages but then exhibits a slower saturation. The diagonal polarised input gives an intermediate behaviour, as it is a mixture of vertical and horizontal polarisation. The general switching behaviour closely resembles a twisted nematic cell, which has been plotted as a reference (for details on the simulation see Section S1, supporting information).

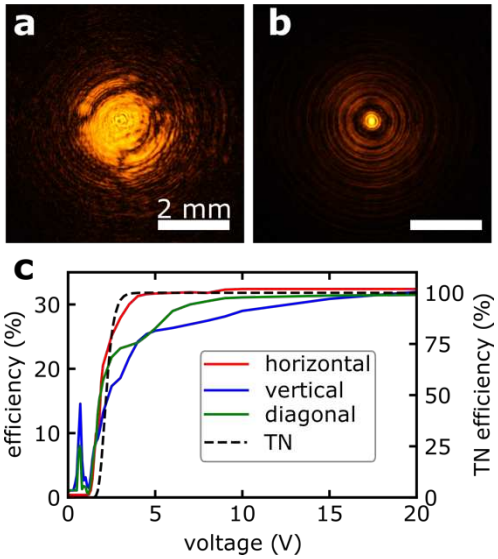

Figure 4. *Transmission of laser beam (594 nm) through Fresnel zone cell on a CCD camera in 20 cm distance: (a) off-state and (b) on-state (10 V). (c) Efficiency of power focused into the central spot for different input polarisations and transmission properties of a twisted nematic (TN) cell modelled according to the lens specification (see section S1 in the supporting information for more information on the modelling).*

Theoretically, an efficiency of ~41 % is expected. Assuming perfect index matching between LC and RM, there are three factors which negatively impact the diffraction efficiency: the profile of the embossed structure, the effects of the sharp edges on the liquid crystal and the alignment quality of the reactive mesogen. From the profile of the embossed RM lens (Figure S1, supporting information), we see that the embossed structure has smaller amplitude than the master, which arise from slight deformation of the mould during embossing. This lowers the phase shift and hence the efficiency. Secondly, the application of a voltages causes some distortions in the LC at the edges of the RM rings as can be seen in the polarising optical images (**Figure S4**, supporting information). Here, the director does not assume a homeotropic configuration, which leads to a residual birefringence. Lastly, the alignment of the RM at the edges is not perfect due to strong spatial variations that lead to high elastic deformations. The imperfections are then transferred to the liquid crystal alignment, as discussed further below.

A detailed investigation of the beam profile is shown in **Figure 5**a. For different applied voltages, a central spot emerges that

increases in intensity. For the different input polarisations (horizontal, vertical, diagonal), there is little variation in intensity or shape. A notable discrepancy, however, is that for the horizontal and the vertical polarisation the spot profile is elongated along the respective polarisation axis. This does not occur for the diagonal input, which fits the device design with the horizontal and vertical axes being principle axes of the lens. A diagonal polarised input is therefore split in equal parts, horizontal and vertical, which compensates the slight ellipticity observed for the pure horizontal and vertical inputs.

Figure 5(b-d) shows the voltage dependent peak intensity of the beam and the beam widths (full width at half maximum, FWHM) for x- and y-cuts for different input polarisations. The peak power density without an output polariser shows very similar behaviour to the efficiency measurements, wherein saturation follows the initial steep increase. The polarisation dependent output measurements show the polarisation conversion due to the TN effect is stopped rapidly after the critical voltage is exceeded, above which the output polarisation corresponds to the input. The reduction of amplitude for the polarised measurements is

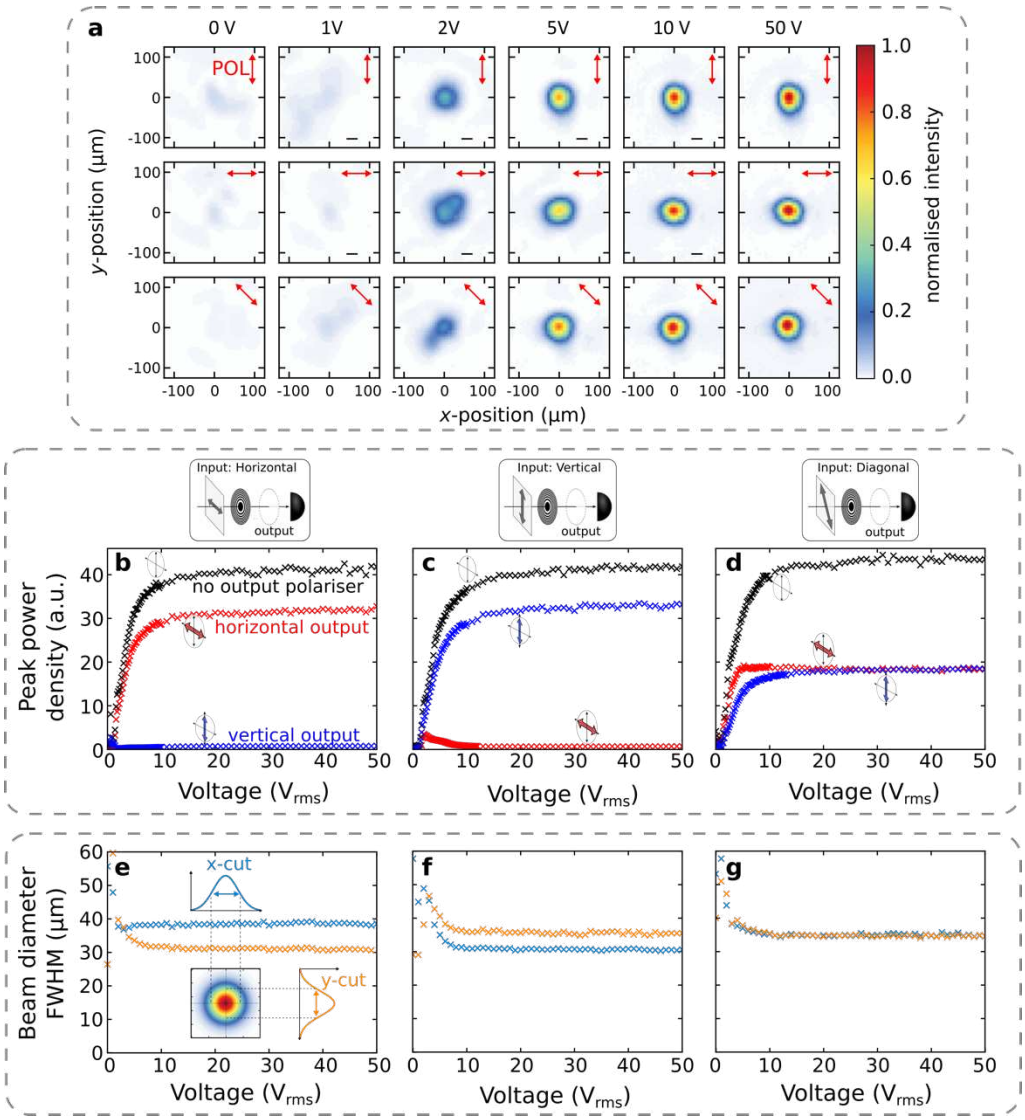

Figure 5. (a) *Beam profiles measured for different input polarisations (red arrow): vertical, horizontal, diagonal at different voltages.* ***(b-d)*** *Peak intensity of central peak for different input and output polarisations as a function of voltage.* ***(e-f)*** *Voltage-dependent spot diameter (full width at half maximum FWHM) for different input polarisations (no output polariser).*

caused by absorption of the employed polariser, which transmits ~80 % of the incoming light. For the diagonal input, the polarised output shows equal parts horizontal and vertical polarised light. The horizontal component saturates faster than the vertical, which already has been observed in the efficiency measurements (Figure 4c). The beam diameter (full width at half maximum, FWHM) (Figure 5e-g) decreases with increasing voltage due to the increased focusing. The ellipticity for the horizontally and vertically polarised input is clearly visible. Also, the compensation for the diagonal input is as expected from the 2D beam profiles (Figure 5a-c). Investigating the absolute values of the FWHM further supports this. For the diagonal, the beam width of 35 µm is very close to the larger diameters, 36 µm and 37 µm, which is found for the horizontal and vertical polarisations. As a comparison, the smaller diameters are about 30 µm. Although the influence of variations in temperature, wavelength and illumination angle were note measured directly, they are anticipated to be small, since numerical calculations show that a large change in LC refractive index (0.015, which is typical of a 10K temperature change) causes less than a 1% change of lens efficiency.

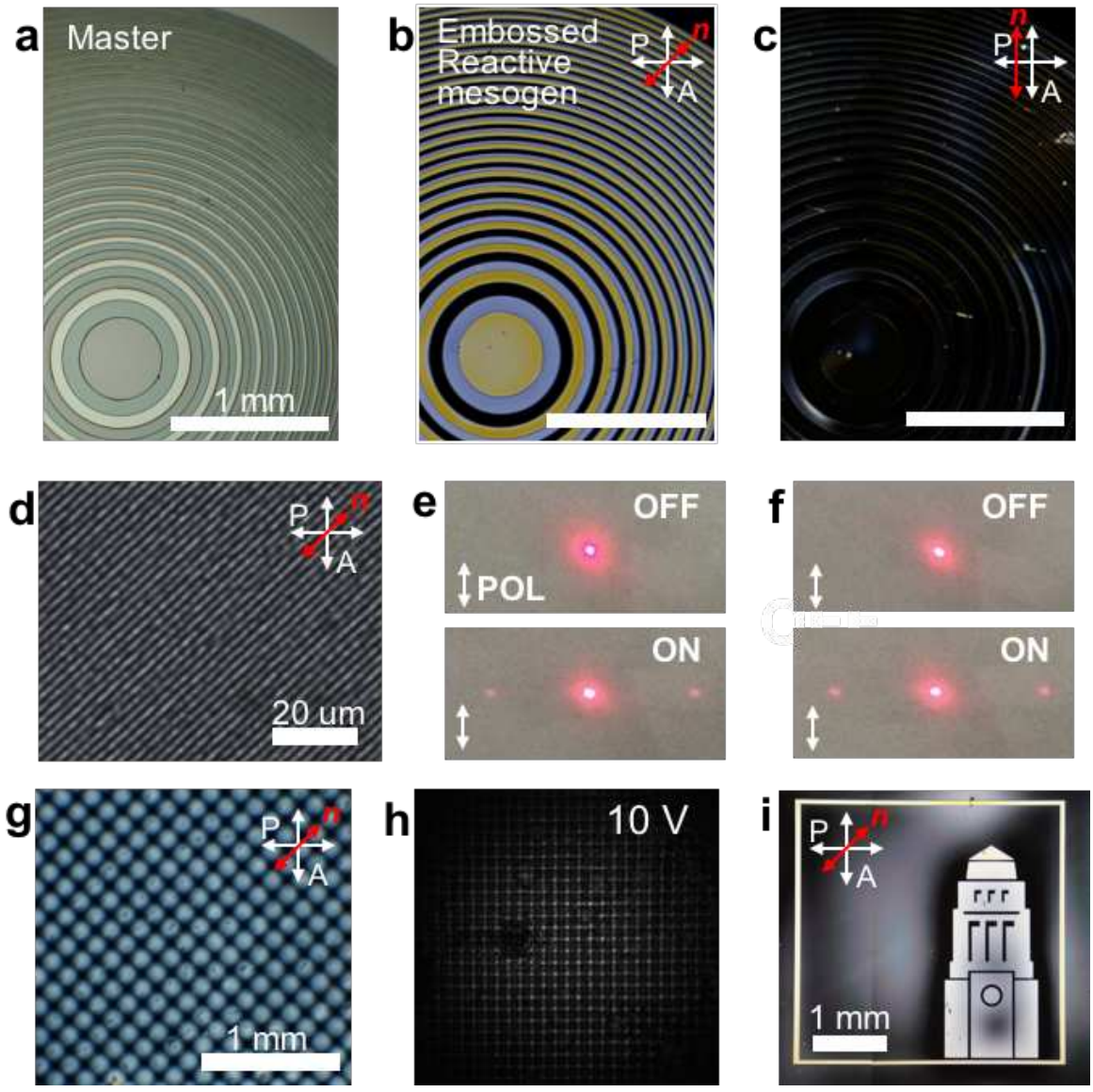

Figure 6. *(a-c) Optical microscope images of three-level Fresnel lens: (a) master on silicon, (b, c) embossed lens substrate between crossed polarisers. (d) Embossed grating (2 um pitch, 125 nm amplitude) between crossed polarisers, (e, f) electrically switchable diffraction for different input polarisations. (g) embossed microlens array (MLA) between crossed polariser, (h) camera image of Gaussian beam focused by MLA cell at 10 V. (i) Embossed University of Leeds logo between crossed polarisers.*

The ellipticity is assumed to be caused by imperfect alignment close to the rims of the RM ringed structures, which transfers to the alignment of the liquid crystal. In a perfectly aligned reactive mesogen Fresnel zone lens, the RM director is uniformly aligned within these ringed structures, which includes regions where the director is perpendicular on the ring edges. In reality however, distortion of the director at these edges is more likely to appear, as the PVA alignment layer treatment of the mould would promote planar anchoring at that position. For horizontally polarised light, this means that along the horizontal axis is less focused due to the decreased index contrast, which leads to an increased spot size along this axis.

As mentioned previously, the technique presented here is not limited to simple Fresnel zone plates but can be used for many types of optical element. First, to overcome the efficiency limitation of binary Fresnel lens we applied the embossing process together with the polarisation-independent design to multilevel Fresnel lenses (**Figure 6**a-c). The measured efficiencies for three-level design is 53 %, which proves that this approach can exceed 50%. This still falls short of the theoretically predicted 68 %, but we believe that by optimizing the technique the devices can get close to this efficiency (see Figure S4 for surface profiles, supporting information). The approach can also be used to replicate existing optical elements, and arrange them to become switchable, polarisation independent structures. Two such examples of reproducing existing optical elements are given in Figure 6d-h. A 1D grating has been embossed into RM (Figure 6d) by using commercially available grating film. In this instance, the process of moulding the master is skipped, since the grating was already on a PET film. Using two RM grating substrates, one with the director parallel to the grating grooves, the other in the orthogonal direction, a switchable polarisation-independent grating has been produced (Figure 6e, f).

Figure 6g displays an aligned-RM replica of a microlens array (MLA). To avoid damage to the MLA, it was first moulded in PDMS and then stamped in a hard resin to obtain a master suitable for further processing. With the standard process, two reactive mesogen reproductions have been made, which were then assembled into a liquid crystal device. Switching the MLA to the ON state is shown in Figure 6h, which shows the focusing of a Gaussian beam with 45° input polarisation with respect to the RM director.

Figure 6i shows a 4mm replication of the University of Leeds logo, the Parkinson tower, into a birefringent RM layer, to illustrate that complex shapes can be produced employing the presented technique.

4. Conclusion

In conclusion, we presented a general method for manufacturing polarisation-independent switchable optical elements. This method relies on embossing the desired structure in optical anisotropic reactive mesogens. As the main example, we presented a polarisation-independent binary Fresnel zone plate with an efficiency of 33 %. To increase the efficiency, we employed a three level Fresnel zone plate reaching a diffraction efficiency of 53%. Even higher efficiencies can be reached by using more levels and finally reaching the analogue modulation of a perfect Fresnel lens. Further, we presented two polarisation-independent devices, which were created from commercially available optical elements: a one-dimensional diffraction grating and a microlens array. One of the limitations of the embossing of reactive mesogens lies in reproducing structures with high spatial frequencies, for example sharp edges as found in Fresnel zone plates and small pitched but high amplitude gratings. Due to the liquid crystalline nature of the embossing material (reactive mesogens), the rapidly changing forms can lead to high elastic energies, which the liquid crystals reduce by assuming the director profile with the lowest energy. The exact limits and methods to expand them are under investigation.

In general, this technique can be used to turn a large variety of passive optical elements into switchable polarisation-independent devices. Most notably, switchable optical lenses can find applications in devices like smartphones, cameras and augmented or mixed reality devices. The benefits of embossing structured reactive mesogens films reach beyond the field of optics and may be used to pattern liquid crystal elastomers to produce for example actuators, which are more

complex than commonly employed planar films.

Data associated with this work are available from the Research Data Leeds repository under a CC-BY license at http://doi.org/10.5518/441.

Experimental Section

Master fabrication: The Fresnel zone plate masters are manufactured by using a direct writing laser system. SU-8 is spin coated on a silicon wafer and processed according to the manufacturer's instruction. The target feature height of 2.1 µm is verified by measuring the surface profile (Dektak XT).

Mould Fabrication: The isotropic resin which is used to mould the master consists of 45% HDDA, 15% TMPTA and 40% Actilane 420. A photoinitiator (Genocure LTM, 4%) is added. The resin is deposited on the master, topped with flexible 125 um thick PET film (Melinex 506) and then cured. After curing, the film with the resin is lifted off. The mould is treated with UV-ozone before spin coating PVA solution (1% in H_2O). The PVA layer is dry rubbed using a rubbing machine equipped with a velvet cloth.

Substrate preparation & embossing: ITO substrates are thoroughly cleaned using different solvents and final UV/ozone treatment. The samples are covered with a solution consisting of polyimide SE 3510 (66 wt%, Nissan Chemicals), dimethylformamide (33 wt%) and reactive mesogen RM257 (1 wt%, Merck) for alignment and adhesion. This solution is spin coated and cured at 180°C for 1h. Finally, the samples are rubbed for planar alignment. For the embossing, a droplet of reactive mesogen mixture RMM1850 (Merck Chemicals Ltd., $\boldsymbol{\Delta n = 0.14}$ **at 589 nm, 25°C**) is deposited at the edge of the ITO substrate and the rubbed mould is placed on top. The reactive mesogen mixture contains photoinitiator sensitive to UV-A radiation. The embossing process is performed at a base plate temperature 85°C, 4.5 bar of roller pressure and substrate speed of 6.5 mm/s. After embossing, the sample is cooled to room temperature within a period of 5 minutes. The sample is UV-cured with a UV-A intensity of 10 mW/cm^2 for 10 minutes. Finally, the film is removed leaving behind the reproduced structure.

Lens assembly & measurement: The normal and complementary Fresnel zone plate substrates are assembled into a cell such that the directors form a 90° angle. The alignment is performed by hand under a microscope to ensure good positioning of the structures. The cell gap is controlled using Mylar spacers and confirmed by multiple measurements of interference fringes close to but outside the Fresnel structure. The cell is sealed on three of the four sides to enable vacuum filling. This method of filling is preferred as capillary filling usually leads to air bubbles being trapped in the cell when using the steeply sided profiled surfaces. The cell is filled with the liquid crystal MLC-6204-000, which has a positive dielectric anisotropy (Table S1, supporting information). After filling and forming electrical contacts, the cell is measured using a HeNe laser (λ = 594 nm). The output state is measured using a beam profiler (Thorlabs BC106N-VIS).

Supporting Information

Supporting Information is available from the Wiley Online Library or from the author.

Acknowledgements

J.C.J. acknowledges the financial support from EPSRC Manufacturing Fellowship EP/L015288/2. The work was conducted under the Leeds and Merck collaboration (LAMP) and M.W. thanks Merck for funding. The authors thank Merck Chemicals Ltd for supplying the reactive mesogen mixture.

References

[1] H. Kikuchi, M. Yokota, Y. Hisakado, H. Yang and T. Kajiyama, *Nat. Mater.* **2002**, *1*, 64.

[2] F. Castles, F. V. Day, S. M. Morris, D-H. Ko, D. J. Gardiner, M. M. Qasim, S. Nosheen, P. J. W. Hands, S. S. Choi, R. H. Friend and H. J. Coles, *Nat. Mater.* **2012** *11*, 599.

[3] C. Ohm, M. Brehmer and R. Zentel, *Adv. Mater.* **2010**, *22*, 3366-3387.

[4] S. Schuhladen, F. Preller, R. Rix, S. Petsch, R. Zentel, and H. Zappe, *Adv. Mater.* **2014**, *42*, 7247.

[5] T. J. White and D. J. Broer, Nature Materials **2015**, *14*, 1087.

[6] H. Zeng, O. M. Wani, P. Wasylczyk, R. Kaczmarek and A. Priimagi, *Adv. Mater.* **2017**, *29*, 1.
[7] W. Wei, Z. Zhang, J. Wei, X. Li and J. Guo, *Adv. Opt. Mater.* **2018**, *6*, 180131.
[8] D.J. Broer, G.P. Crawford and S. Žumer, Cross-linked Liquid Crystalline Systems, **2011**, *CRC Press, Boca Raton, FL, USA*.
[9] Y. Sawa, K. Urayama, T. Takigawa, A. DeSimone, and L. Teresi, *Macromolecules* **2010**, *43*, 4362.
[10] C. C. Tartan, P. S. Salter, T. D. Wilkinson, M. J. Booth, S. M. Morris and S. J. Elston, *RSC Adv*. **2017**, *7*, 507.
[11] C. C. Tartan, J. J. Sandford O'Neill, P. S. Salter, J. Aplinc, M. J. Booth, M. Ravnik, S. M. Morris and S. J. Elston, *Adv. Opt. Mater.* **2018,** 1800515.
[12] S. Y. Chou, P. R. Krauss, and P. J. Renstrom, Appl. Phys. Lett. **1995,** *67,* 3114.
[13] R.M. Amos, G. P. Bryan-Brown, E. L. Wood, J.C. Jones and P. T. Worthing, **2003,** US patent # 7,824,516, B2.
[14] J. C. Jones, *J. Soc. Inf. Disp.* **2008**, *16*, 143.
[15] J.C. Jones and M. Wahle, **2018**, GB patent application.
[16] I.M. Syed, S. Kaur, H.E. Milton, D. Mistry, J. Bailey, P.B. Morgan J.C. Jones and H.F. Gleeson, *Optics Express*, **2015,** 23, 9911-9916.
[17] J. Bailey, P. Morgan, H. Gleeson and J. C. Jones, *Crystals* **2018**, *8*, 1.
[18] U. Li, J. Peng, F. Pab, Y. Wu, Y. Zhang and X. Xie, *Opt. Express*, **2018**, *10*, 12441.
[19] Y.-J. Wang, P.-J. Chen, X. Liang and Y.-H. Lin, *Sci. Rep.* **2017**, *7*, 433.
[20] S. Sato, *Jap. J. Appl. Phys.* **1979**, *18*, 1679.
[21] S. Masuda, S. Takahashi, T. Nose, S. Sato, and H. Ito, *Appl. Opt.* **1997**, *36*, 4772.
[22] L. Li, D. Bryant, T. Van Heugten and P. J. Bos, *Opt. Express* **2013**, *21*, 8371.
[23] A. Y.-G. Fuh, S.-W. Ko, S.-H. Huang, Y.-Y. Chen and T.-H. Lin, *Opt. Express* **2011**, *19*, 2294.
[24] Z. Xin, Q. Tong, Y. Lei, D. Wei, X. Zhang, J. Liao, H. Wang, and C. Xie, *J. Opt.* **2017**, *19*, 095602.
[25] H. Ren, Y. H. Fan, Y. H. Lin and S. T. Wu, *Opt. Comm.* **2005**, *247*, 101.
[26] D. M. Lee, Y. J. Lee, H. B. Park, C. Jae Yu and J. H. Kim, *Mol. Cryst. Liq. Cryst.* **2017**, *647*, 44.
[27] Y.-H. Lin, H.-S. Chen, H.-C. Lin, Y.-S. Tsou, H.-K. Hsu and W.-Y. Li, *Appl. Phys. Lett.* **2010**, *96*, 113505.
[28] C.-T. Lee, Y. Li, H.-Y. Lin and S.-T. Wu, *Opt. Express* **2011**, *19*, 17402.
[29] T.-H. Lin, Y. Huang, A. Y. G. Fuh and S.-T. Wu, *Opt. Express* **2006**, *14*, 2359.
[30] D. W. Kim, C. Jae Yu, H. R. Kim, S. J. Kim and S. D. Lee, *Appl. Phys. Lett.* **2006**, *88*, 1.
[31] X. Q. Wang, F. Fan, T. Du, A. M. W. Tam, Y. Ma, A. K. Srivastava, V. G. Chigrinov, and H. S. Kwok, *Appl. Opt.* **2014,** *53*, 2026.
[32] C.H. Gooch and H. A. Tarry, *J. Phys. D: Appl. Phys.* **1975,** *8*, 1575 – 1583.

Embossing of reactive mesogens (RMs) is used for manufacturing polarisation-independent optics. The general technique is applied to produce switchable Fresnel zones plates. It is shown that efficiencies beyond 50% can be reached – independent of the polarisation. Further, examples for polarisation-independent gratings and microlens arrays are shown to prove the wide range of applicability of the presented technique.

Keyword: embossing of reactive mesogens

M. Wahle, B. Snow, J. Sargent and J. C. Jones*

Embossing Reactive Mesogens: A Facile Approach to Polarisation-Independent Liquid Crystal Devices

ToC figure ((Please choose one size: 55 mm broad × 50 mm high **or** 110 mm broad × 20 mm high. Please do not use any other dimensions))

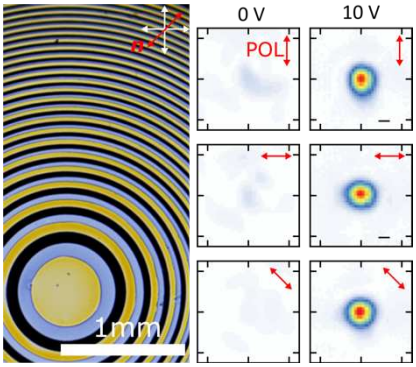

Supporting Information

Embossing Reactive Mesogens: A Facile Approach to Polarisation-Independent Liquid Crystal Devices

*Markus Wahle, Ben Snow, Joe Sargent and J. Cliff Jones**

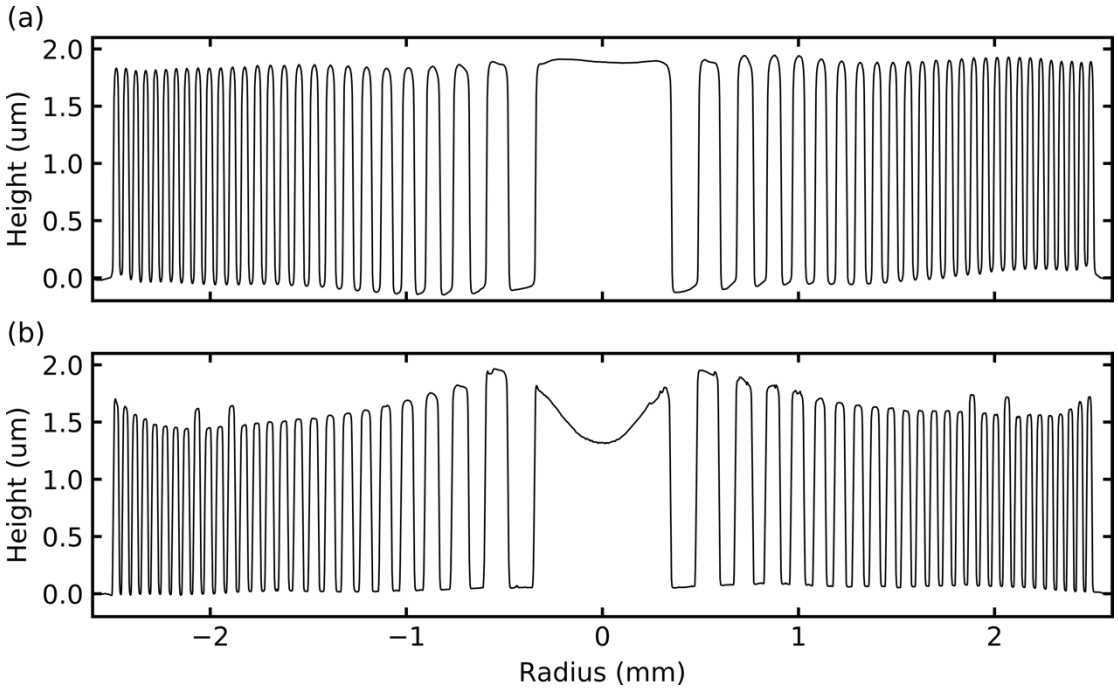

Figure S1: Surface profiles of normal two-level Fresnel lens: (a) Master fabricated in SU-8 on silicon, (b) reproduction in reactive mesogen (RM).

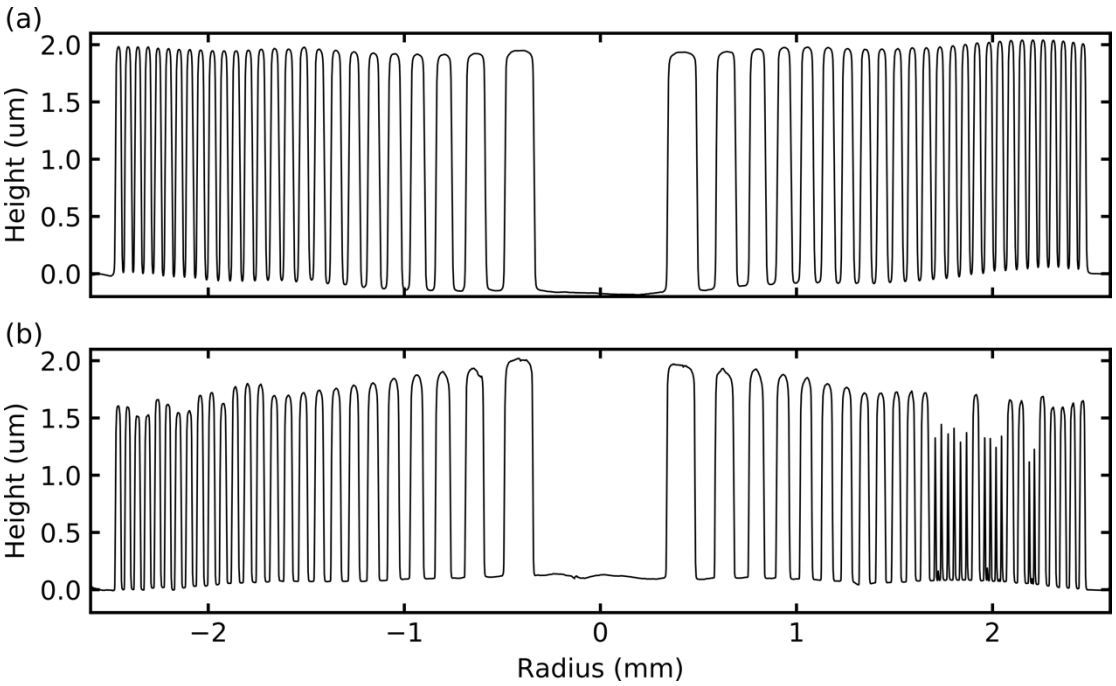

Figure S2: Surface profiles of complementary two-level Fresnel lens: (a) Master fabricated in SU-8 on silicon, (b) reproduction in reactive mesogen (RM).

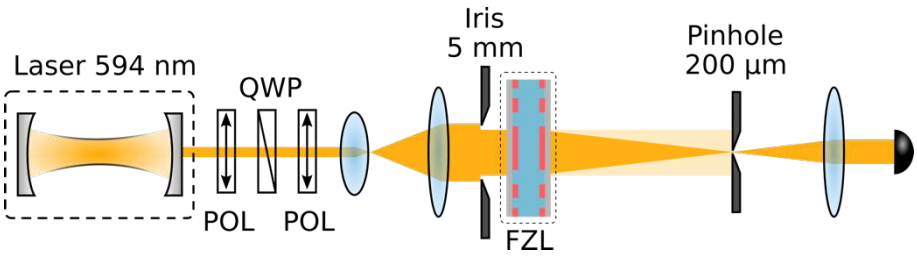

Figure S3: Setup for measuring the diffraction efficiency of Fresnel lenses (POL: polariser, QWP: quarter wave plate, FZL: Fresnel Zone Lens, PD: photo diode).

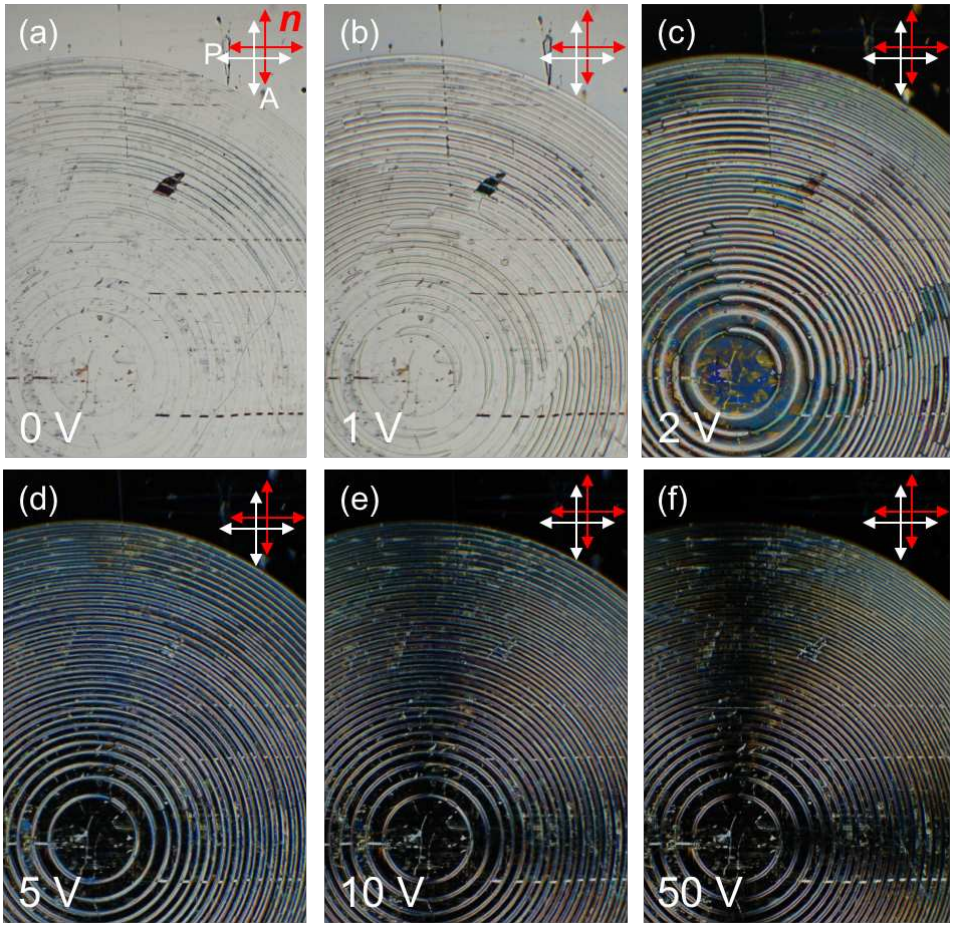

Figure S4: Liquid crystal-filled two-level Fresnel lens between crossed polarisers at different voltages (0 V-50 V). The director $\boldsymbol{n}$ (optical axis) of the reactive mesogen is aligned parallel to polariser (P)/analyser (A).

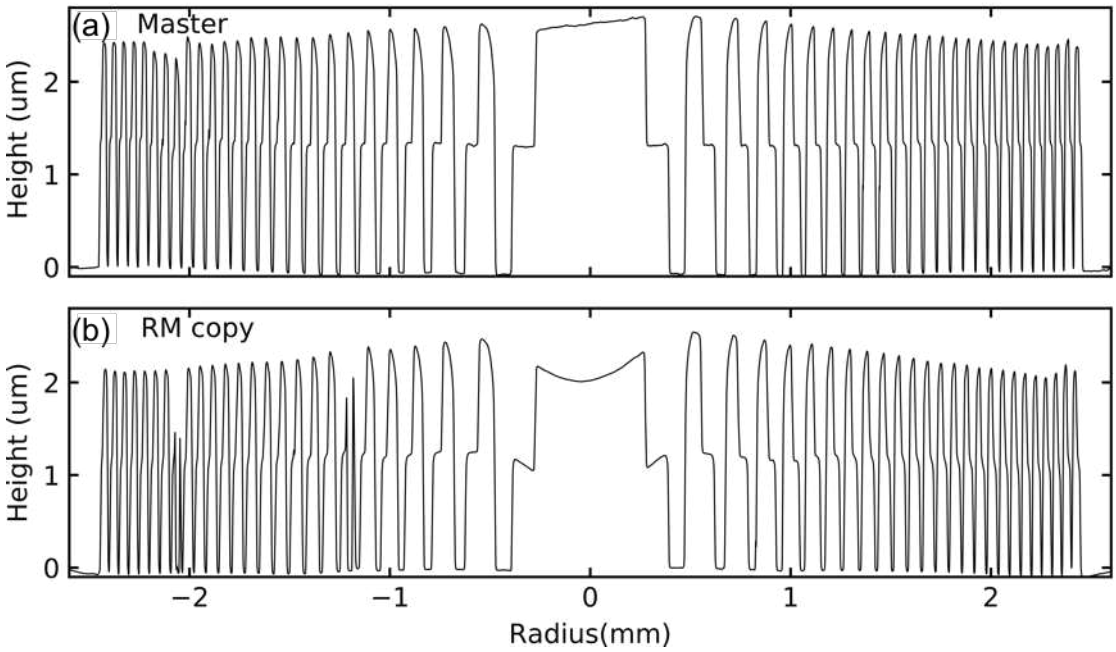

Figure S3: Surface profiles of three level Fresnel lens: (a) Master fabricated in SU-8 on silicon, (b) reproduction in reactive mesogen (RM).

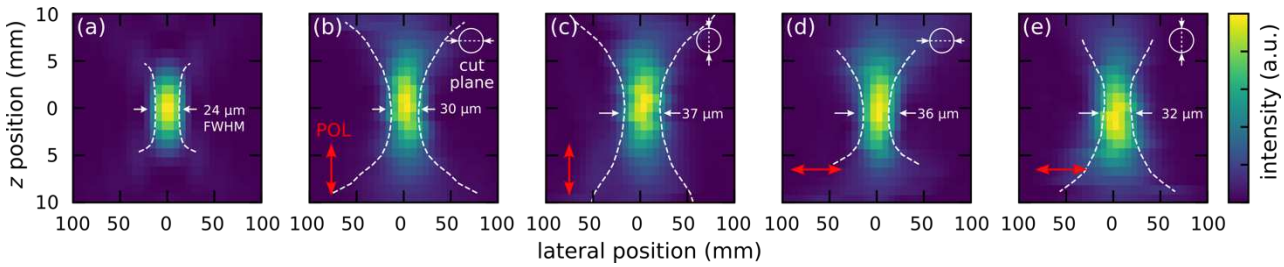

Figure S4: *z*-scans of the point spread function for Fresnel lens (a) simulated, (b-e) experimentally determined at 10 V. Input polarisation: (b, c) horizontally, (d, e) vertically.

Table S1: Physical properties of the liquid crystal (MLC6204-000) and the used for simulation. The refractive indices were measured at 589 nm and 25°C.

Property	**MLC-6204-000**	**RMM1850**
Elastic constant K_{11}	6.0	-
Elastic constant K_{22}	4.3 (estimated)	-
Elastic constant K_{33}	15.2	-
Dielectric constant parallel $\epsilon_{\parallel}$	44.8	-
Dielectric constant perpendicular $\epsilon_{\perp}$	9.5	3.68 (cured)
Ordinary refractive index n_{o}	1.504	1.510 (uncured)
Extraordinary refractive index n_{e}	1.652	1.654 (uncured)

S1 Director field simulation

The director profile was calculated using COMSOL Multiphysics 5.3. The Free energy

$$2F(z) = K_{11}(n_z')^2 + K_{22}\left(n_y n_z' - n_x n_y\right)^2 + K_{33}\left[n_z^2\left(n_x' + n_y'\right) + \left(n_x n_x' + n_y n_y'\right)^2\right] - E_z^2\epsilon_0(\Delta\epsilon n_z^2 + \epsilon_{\perp}) \quad \text{(S1)}$$

was implemented as the weak form with strong anchoring conditions. Here, n_i are the components of the director $n = \left[n_x, n_y, n_z\right]^{\mathrm{T}}$ in Cartesian coordinates ($i = x, y, z$), K_{jj} are the elastic constants ($j = 1,2,3$). E_z designates the electric field in z-direction, ϵ_0 the vacuum permittivity, $\Delta\epsilon$ the dielectric anisotropy and $\epsilon_{\perp}$ the perpendicular permittivity of the liquid crystal. The director field was then used to calculate the transmission of linear polarised light by applying the Jones formalism.